Percolation thresholds for discorectangles: Numerical estimation for a range of aspect ratios

Yuri Yu. Tarasevich [*] and Andrei V. Eserkepov[†]

Laboratory of Mathematical Modeling, Astrakhan State University, Astrakhan 414056, Russia

Using Monte Carlo simulation, we have studied the percolation of discorectangles. Also known as stadiums or two-dimensional spherocylinders, a discorectangle is a rectangle with semicircles at a pair of opposite sides. Scaling analysis was performed to obtain the percolation thresholds in the thermodynamic limits. We found that (i) for the two marginal aspect ratios $\varepsilon = 1$ (disc) and $\varepsilon \to \infty$ (stick) the percolation thresholds coincide with known values within the statistical error and (ii) for intermediate values of ε the percolation threshold lies between the percolation thresholds for ellipses and rectangles and approaches the latter as the aspect ratio increases.

I. INTRODUCTION

Percolation, i.e., the emergence of a connected subset (a cluster) that spans opposite boundaries in a disordered medium, has attracted the attention of the scientific community for several decades [1–5]. The occurrence of a percolation cluster drastically changes the physical properties of the medium, e.g., an insulator-conductor phase transition can be observed when the disordered medium is a mixture of conductive and insulating substances. Special attention has been paid to percolation in disordered systems produced by the random deposition of elongated particles onto a substrate [6–9]. Elongated species such as nanotubes, nanowires, and nanorods are of particular interest for nanotechnology, e.g., the production of transparent electrodes [10–16].

To characterize a deposit, the number density, i.e., the number of objects, N, per unit area, A, is commonly used:

$$n = \frac{N}{A}. \tag{1}$$

Another useful quantity is the filling fraction:

$$\eta = na, \tag{2}$$

where a is the area of one particle. The total fraction of the plane covered by the overlapping (penetrable) particles is

$$\phi = 1 - \exp(-\eta) \tag{3}$$

(see, e.g., [7]).

To mimic the shape of elongated particles and, at the same time, simplify the simulations, different simple geometrical figures are used, e.g., sticks, rectangles, ellipses, superellipses, and discorectangles. A discorectangle is a rectangle with semicircles at a pair of opposite sides (Fig. 1). Its aspect ratio is

$$\varepsilon = 1 + \frac{l}{2r}. \tag{4}$$

A discorectangle (or "stadium") is a two-dimensional analog of a spherocylinder (a "stadium of revolution" or "capsule"), i.e., a three-dimensional geometric shape consisting of a cylinder with hemispherical ends.

Percolation thresholds of two-dimensional continuum systems of rectangles [8] and ellipses [9] for a wide range of aspect ratios from $\varepsilon = 1$ to 1000 have been reported. Both ellipses and rectangles transform into sticks when $\varepsilon = \infty$. When $\varepsilon = 1$, a rectangle is simply a square, while an ellipse is a disk. Currently, the best known value of the percolation threshold of zero-width sticks of equal length that are randomly oriented and placed onto a plane is $n_c^{\times} = 5.637\,285\,8(6)$ [7]. By convention, the value of a for sticks is taken as equal to l^2, where l is the length of the stick. The best known value of the percolation threshold of discs, i.e., ellipses with $\varepsilon = 1$, is $\eta_c^{\circ} = 1.128\,087\,37(6)$, respectively, $n_c^{\circ} = \eta_c^{\circ}/(\pi r^2) = 1.436\,325\,45(8)$ [7]. A calculation has been presented for the excluded area between penetrable rectangles in two dimensions as a function of the aspect ratio and orientational order parameter [17]. The percolation threshold was found to rise with increases in the degree of particle alignment. For isotropically distributed systems, the percolation thresholds for different values of the aspect ratio are in close agreement with findings from Monte Carlo simulations [8]. Recently, percolation thresholds of superellipses have been reported [18]. In a Cartesian coordinate system, the equation of a superellipse is

$$\frac{|x|^{2m}}{a^{2m}} + \frac{|y|^{2m}}{b^{2m}} = 1, \tag{5}$$

where a and b are the semimajor lengths in the direction of the x and y axes and m is the shape parameter. $m = 1$ corresponds to an ellipse while $m = +\infty$ corresponds to a rectangle. Percolation thresholds as the total fractions of the plane covered by the particles, ϕ_c, have been presented for 14 shapes, for each of six aspect ratios [18].

Although the percolation of spherocylinders has been studied [19], to the best of our knowledge, the percolation thresholds for their two-dimensional analogs, i.e.,

---
[*]Corresponding author: tarasevich@asu.edu.ru
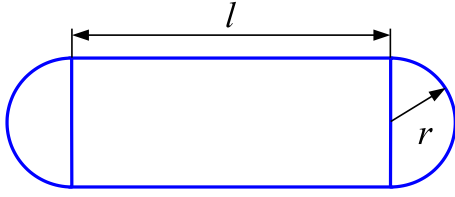[†]dantealigjery49@gmail.com

FIG. 1. Example of a discorectangle.

discorectangles, have not yet been presented in the literature. The goal of the present paper was to obtain the dependencies of the percolation thresholds of randomly placed and oriented discorectangles on their aspect ratios. The rest of the paper is constructed as follows. In Sec. II, the technical details of the simulations and calculations are described. Section III presents our main findings. Section IV summarizes the main results.

II. METHODS

We used the union-find algorithm [20,21] to check for any occurrences of wrapping clusters. In our study, we used the version of the union-find algorithm adapted for continuous percolation [6,7].

Discorectangles with $l = 1$ were added one by one randomly, uniformly, and isotropically onto a substrate of size $L \times L$ having periodic boundary conditions, i.e., onto a torus, until a cluster wrapping around the torus in two directions had arisen. In this case, the desired number density, n, is

$$n = \frac{N}{L^2}. \tag{6}$$

Intersections of the discorectangles were allowed (Fig. 2). For each given system size, L, and number of deposited discorectangles, N, 10^5 independent runs were performed to obtain the probability of percolation, $R_{N,L}^{(c)}$. Here, the superscript c means a used criterion; viz., h, v, or b means that the cluster winds the torus in the horizontal direction, in the vertical direction, or in both directions, respectively.

To obtain the probability $R^{(c)}(\eta, L)$ of percolation in the grand canonical ensemble, we convolved $R_{N,L}^{(c)}$ with the Poisson distribution [6,7]:

$$R^{(c)}(\eta, L) = \sum_{N=0}^{\infty} \frac{\lambda^N e^{-\lambda}}{N!} R_{N,L}^{(c)}. \tag{7}$$

The weights in Eq. (7) $w_N(\lambda) = \lambda^N / N!$ can be calculated using the recurrent relations [7],

$$w_{\bar{N}-k} = \begin{cases} 1, & \text{for } k = 0, \\ \frac{\bar{N}-k+1}{\lambda} w_{\bar{N}-k+1}, & \text{for } k = 1, 2, \ldots, \end{cases} \tag{8}$$

and

$$w_{\bar{N}+k} = \begin{cases} 1, & \text{for } k = 0, \\ \frac{\lambda}{\bar{N}+k} w_{\bar{N}+k-1}, & \text{for } k = 1, 2, \ldots, \end{cases} \tag{9}$$

where the relation

$$\sum_{N=0}^{\infty} \frac{\lambda^N}{N!} = \sum_{N=0}^{\infty} w_N(\lambda) = e^\lambda, \quad \forall \lambda > 0$$
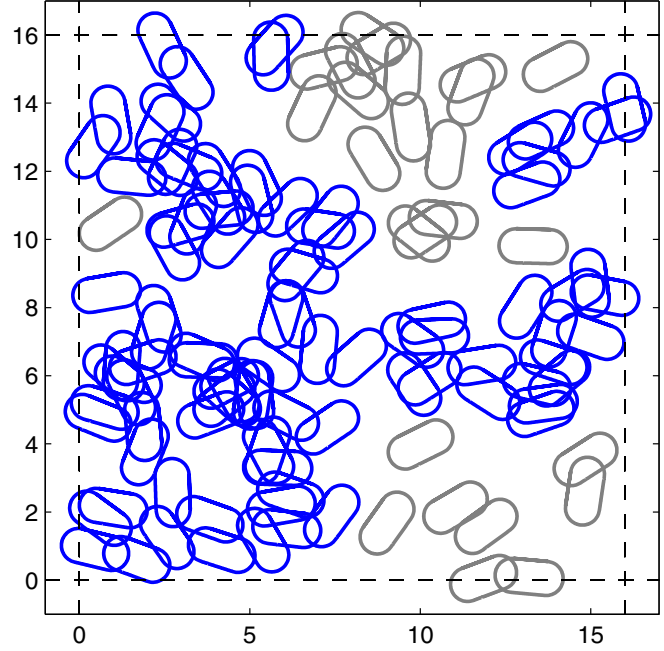

FIG. 2. Example of a system of discorectangles ($\varepsilon = 2$) exactly at the percolation threshold. The linear system size is $16l$. The incipient wrapping cluster is highlighted.

should be borne in mind. Here, $\bar{N} = \lfloor \lambda \rfloor$. Therefore, the convolution can be calculated as

$$R^{(c)}(\eta, L) = \sum_{N=0}^{\infty} w_N^*(\lambda) R_{N,L}^{(c)}, \tag{10}$$

where

$$w_N^*(\lambda) = \frac{w_N(\lambda)}{\sum_{N=0}^{\infty} w_N(\lambda)}. \tag{11}$$

The factor $e^{-\lambda}$ is absent in the master equation (10), since

$$\sum_{N=0}^{\infty} w_N(\lambda) = e^\lambda \sum_{N=0}^{\infty} w_N^*(\lambda).$$

Conformal field theory gives exact values for the wrapping probabilities at the transition in the limit $L \to \infty$ [20–22]:

$$R_\infty^{(c)} = \begin{cases} 0, & \text{if } \eta < \eta_c, \\ R^*, & \text{if } \eta = \eta_c, \\ 1, & \text{if } \eta > \eta_c, \end{cases} \tag{12}$$

where $R^* = 0.521\,058\,290\ldots$ is the probability of wrapping horizontally around the system and $R^* = 0.351\,642\,855\ldots$ is the probability of wrapping around both directions simultaneously. More precise values of R^* including other possible criteria are presented in Ref. [7]. This theory provides the most effective method for estimating the percolation threshold [6,7,20,21] since

$$\eta_c(\infty) - \eta_c(L) \propto L^{-2-1/\nu}, \quad \text{where } \nu = 4/3. \tag{13}$$

Typically, we used systems of sizes $L = 8, 16, 32, 64$ to perform the scaling analysis. The number of independent runs
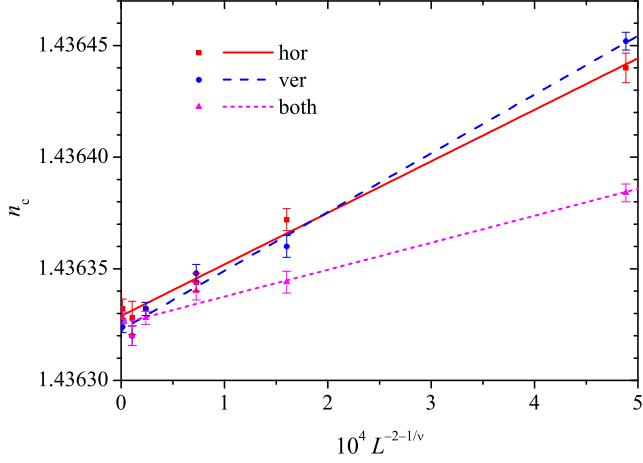
FIG. 3. Example of scaling for discs, i.e., discorectangles with $\varepsilon = 1$.

was 10^5. All results presented in Sec. III correspond to the thermodynamic limit.

To verify our program, we performed more accurate estimations for one particular case, viz., $\varepsilon = 1$ (discs of $r = 1/2$). For this particular case, we used $L = 16, 24, 32, 48, 64, 128$ while the number of independent runs was 10^9 for $L \leqslant 48$ and 10^8 for $L > 48$ (Fig. 3).

Figure 3 demonstrates an example of scaling for $\varepsilon = 1$. According to Ref. [7], the standard deviation was taken as $\approx N_{ir}^{-1/2} L^{-3/4}$, where N_{ir} is the number of independent runs. Our estimations gave $n_c^\circ = 1.436\,327(7)$ with the adjusted $R^2 = 0.98$. This estimation is reasonably close to the published values for discs of unit diameter $n_c^\circ = 1.436\,323(3)$ [9] and $1.436\,325\,45(8)$ [7]. $n_c^\circ = 1.436\,322(3)$ [23] and $1.436\,32(5)$ [24].

Additionally, we checked the derivative of R at the percolation threshold. An example of the dependency of $R'(L)$ for wrapping in the horizontal direction is presented in Fig. 4
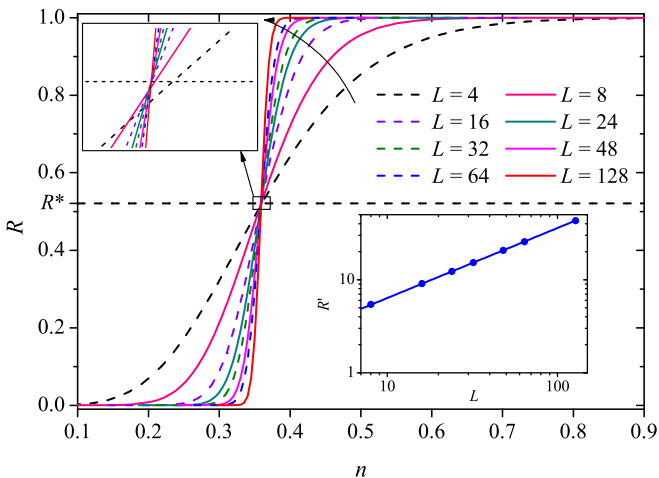

FIG. 4. $R(n)$ for different system sizes. The curved arrow indicates increasing of L. Inset: Example of the dependency of $R'(L)$ for wrapping in the horizontal direction in log-log scale.

TABLE I. Comparison of the percolation thresholds of rectangles n_c^r [8], ellipses n_c^e [9], and discorectangles (our results) for different values of the aspect ratio. Case $\varepsilon = \infty$ corresponds to the percolation of sticks [7]. The values are rounded to significant figures.

ε	n_c^r	n_c^{DR}	n_c^e
1	0.982278	1.436	1.436323
1.5	1.425745	1.894	2.059081
2	1.786294	2.245	2.523560
3	2.333491	2.760	3.157339
4	2.731318	3.123	3.569706
5	3.036130	3.396	3.861262
6	3.278680	3.612	4.079359
7	3.477211	3.787	4.249158
8	3.643137	3.933	4.385303
9	3.784321	4.057	4.497044
10	3.906022	4.163	4.590416
15	4.329848	4.530	4.894745
20	4.584535	4.749	5.062313
30	4.878091	5.000	5.241522
50	5.149008	5.229	5.393863
100	5.378856	5.422	5.513464
200	5.504099		5.612260
1000	5.609947		5.624756
∞		5.6372858	

(inset) in log-log scale. The slope is 0.752 ± 0.002 and this corresponds to the value of the critical exponent ν.

III. RESULTS

Our results are presented in Table I, which compares the percolation thresholds for discorectangles (our results) with
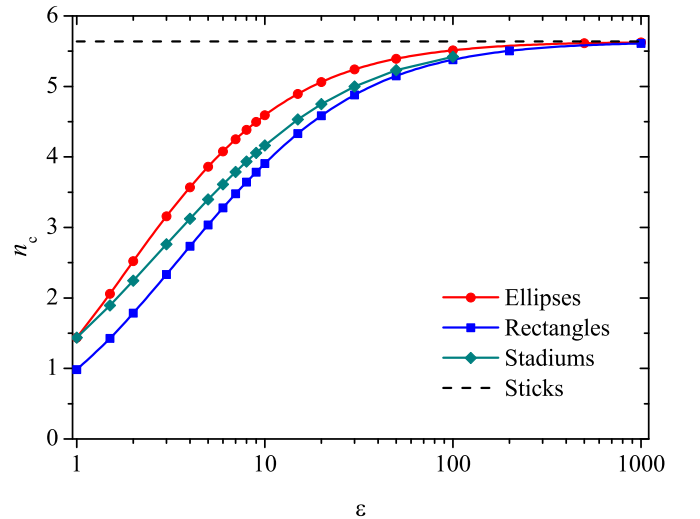

FIG. 5. Dependencies of the percolation threshold, n_c, on the aspect ratio, ε, for rectangles [8], ellipses [9], and discorectangles (our results) in a semilog plot with a logarithmic scale on the ε axis, and a linear scale on the n_c axis. The horizontal dashed line corresponds to the percolation of sticks ($\varepsilon = \infty$) [7]. The error bars are of the order of the marker size when not shown explicitly.
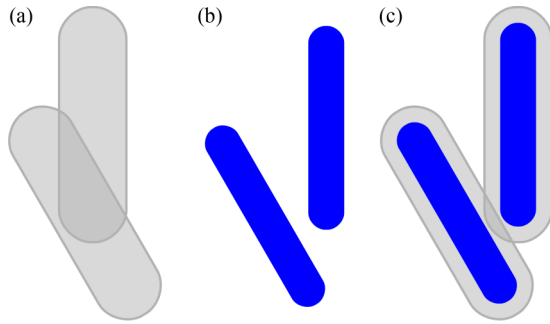
FIG. 6. Permeable (a) and hard-core soft-shell (c) particles can form a cluster while impermeable particles (b) cannot.

known values for rectangles n_c^r [8] and ellipses n_c^e [9] for different values of the aspect ratio.

Figure 5 demonstrates the dependencies of the percolation threshold, n_c^{DR}, on the aspect ratios of discorectangles, ε. The dependencies for rectangles $n_c^r(\varepsilon)$ [8] and ellipses $n_c^e(\varepsilon)$ [9] are shown for comparison. For any value of ε, the critical number density increases as the aspect ratio increases. When $\varepsilon = 1$, the discorectangle is simply a disk; hence, the percolation threshold of such discorectangles equals the percolation threshold of discs. When $\varepsilon \to \infty$, ellipses, rectangles, and discorectangles all tend to sticks. Thus their percolation thresholds approach the percolation threshold of zero-width sticks. For any values of ε, the percolation threshold of discorectangles is situated between the percolation thresholds of ellipses (upper boundary) and rectangles (lower boundary).

IV. CONCLUSION

By means of computer simulation and scaling analysis, we studied the percolation of discorectangles on a torus. The

dependencies of the percolation threshold, n_c^{DR}, on the aspect ratio, ε, have been obtained in the thermodynamic limit. Comparison with known results for rectangles [8], n_c^r, and ellipses [9], n_c^e, evidenced that

$$n_c^r(\varepsilon) < n_c^{DR}(\varepsilon) \leqslant n_c^e(\varepsilon).$$

Naturally, $n_c^{DR}(0) = n_c^e(0)$ since, in this case, each of these shapes is simply a disk. The value of $n_c^{DR}(\varepsilon)$ tends to the value n_c for zero-width sticks [7] when $\varepsilon \to \infty$. Improvements to the accuracy of the obtained values of the percolation threshold will require additional time and computational resources.

Our consideration deals with only one particular case when overlapping of particles is allowed. If the particles are treated as permeable, overlapped particles form a cluster [Fig. 6(a)]. However, other possibilities are also feasible. For instance, in random sequential adsorption [25], particles are impermeable and no cluster can occur [Fig. 6(b)].

An intermediate possibility is the so-called connectedness percolation of nonoverlapping particles [26,27]. Two nonoverlapping particles are assumed to be connected when the shortest distance between them does not a exceed a certain value, i.e., the so-called cutoff distance [28]. This case can be also treated as a hard-core soft-shell model [Fig. 6(c)]. Naturally, in this case, the percolation threshold has to significantly depend on the cutoff distance.

Both length dispersity and alignment of particles may affect the percolation threshold [26,29,30]. In the case of permeable discorectangles, these effects require additional examination.

[1] D. Stauffer and A. Aharony, *Introduction to Percolation Theory*, 2nd ed. (Taylor & Francis, London, 1994).

[2] M. Sahimi, *Applications of Percolation Theory* (Taylor & Francis, London, 1994).

[3] B. Bollobás and O. Riordan, *Percolation* (Cambridge University, Cambridge, England, 2006).

[4] G. R. Grimmett, *Percolation* (Springer-Verlag, Berlin, 1999).

[5] H. Kesten, *Percolation Theory for Mathematicians*, Progress in Probability and Statistics Vol. 2 (Birkhäuser, Boston, 1982), pp. iv and 423.

[6] J. Li and S.-L. Zhang, Finite-size scaling in stick percolation, Phys. Rev. E **80**, 040104(R) (2009).

[7] S. Mertens and C. Moore, Continuum percolation thresholds in two dimensions, Phys. Rev. E **86**, 061109 (2012).

[8] Jiantong Li and M. Östling, Percolation thresholds of two-dimensional continuum systems of rectangles, Phys. Rev. E **88**, 012101 (2013).

[9] Jiantong Li and M. Östling, Precise percolation thresholds of two-dimensional random systems comprising overlapping ellipses, Physica A **462**, 940 (2016).

[10] D. S. Hecht, L. Hu, and G. Irvin, Emerging transparent electrodes based on thin films of carbon nanotubes, graphene, and metallic nanostructures, Adv. Mater. **23**, 1482 (2011).

[11] V. B. Nam and D. Lee, Copper nanowires and their applications for flexible, transparent conducting films: A review, Nanomaterials **6**, 47 (2016).

[12] T. Ackermann, R. Neuhaus, and S. Roth, The effect of rod orientation on electrical anisotropy in silver nanowire networks for ultra-transparent electrodes, Sci. Rep. **6**, 34289 (2016).

[13] C. O'Callaghan, C. Gomes da Rocha, H. G. Manning, J. J. Boland, and M. S. Ferreira, Effective medium theory for the conductivity of disordered metallic nanowire networks, Phys. Chem. Chem. Phys. **18**, 27564 (2016).

[14] D. McCoul, W. Hu, M. Gao, V. Mehta, and Q. Pei, Recent advances in stretchable and transparent electronic materials, Adv. Electron. Mater. **2**, 1500407 (2016).

[15] C. Zhang, Y. Zhu, P. Yi, L. Peng, and X. Lai, Fabrication of flexible silver nanowire conductive films and transmittance improvement based on moth-eye nanostructure array, J. Micromech. Microeng. **27**, 075010 (2017).

[16] J. Hicks, J. Li, C. Ying, and A. Ural, Effect of nanowire curviness on the percolation resistivity of transparent, conductive metal nanowire networks, J. Appl. Phys. **123**, 204309 (2018).

[17] A. P. Chatterjee, Percolation thresholds and excluded area for penetrable rectangles in two dimensions, J. Stat. Phys. **158**, 248 (2015).

[18] J. Lin and H. Chen, Measurement of continuum percolation properties of two-dimensional particulate systems comprising congruent and binary superellipses, Powder Technol. **347**, 17 (2019).

[19] W. Xu, X. Su, and Y. Jiao, Continuum percolation of congruent overlapping spherocylinders, Phys. Rev. E **94**, 032122 (2016).

[20] M. E. J. Newman and R. M. Ziff, Efficient Monte Carlo Algorithm and High-Precision Results for Percolation, Phys. Rev. Lett. **85**, 4104 (2000).

[21] M. E. J. Newman and R. M. Ziff, Fast Monte Carlo algorithm for site or bond percolation, Phys. Rev. E **64**, 016706 (2001).

[22] H. T. Pinson, Critical percolation on the torus, J. Stat. Phys. **75**, 1167 (1994).

[23] J. A. Quintanilla and R. M. Ziff, Asymmetry in the percolation thresholds of fully penetrable disks with two different radii, Phys. Rev. E **76**, 051115 (2007).

[24] K. Meeks, J. Tencer, and M. L. Pantoya, Percolation of binary disk systems: Modeling and theory, Phys. Rev. E **95**, 012118 (2017).

[25] J. W. Evans, Random and cooperative sequential adsorption, Rev. Mod. Phys. **65**, 1281 (1993).

[26] R. H. J. Otten and P. van der Schoot, Connectivity percolation of polydisperse anisotropic nanofillers, J. Chem. Phys. **134**, 094902 (2011).

[27] T. Drwenski, R. van Roij, and P. van der Schoot, Connectedness percolation of hard convex polygonal rods and platelets, J. Chem. Phys. **149**, 054902 (2018).

[28] S. B. Lee and S. Torquato, Pair connectedness and mean cluster size for continuum-percolation models: Computer-simulation results, J. Chem. Phys. **89**, 6427 (1988).

[29] R. H. J. Otten and P. van der Schoot, Continuum Percolation of Polydisperse Nanofillers, Phys. Rev. Lett. **103**, 225704 (2009).

[30] Y. Yu. Tarasevich and A. V. Eserkepov, Percolation of sticks: Effect of stick alignment and length dispersity, Phys. Rev. E **98**, 062142 (2018).